Regional-scale landslide susceptibility assessment for the hilly state of Uttarakhand, NW Himalaya, India

Vikram Gupta[1],*, Sandeep Kumar[1], Ramandeep Kaur[1] and Ruchika S Tandon[2]

[1]*Wadia Institute of Himalayan Geology, Dehradun, Uttarakhand 248 001, India.*
[2]*Graphic Era Deemed to be University, Dehradun, Uttarakhand 248 001, India.*
*Corresponding author. e-mail: vgupta_wihg@yahoo.com

Landslide and related mass movement activities are common and one of the most destructive natural hazards in the mountainous terrain including the Himalayas. Of the 11 administrative states in the Indian Himalayan region, the state of Uttarakhand has witnessed enhanced activities of these phenomena. It is therefore essential to understand the regional scale landslide susceptibility assessment of the state and in the present study, landslide susceptibility mapping for the entire state has been carried out using bivariate weight of evidence and information value methods which depict that around 51% of the area is located in the high and very high landslide susceptible zones, 22–23% in the moderate and $\sim$26–27% in the low and very low landslide susceptible zones, and slopes ranging between 40° and 60°, located at an elevation of 2000–4000 m, facing towards southern sides and covered with limestone, gneiss, quartzite and phyllite, have higher propensity towards development of landslides in the region.

Keywords. Landslide; susceptibility; Uttarakhand; Himalaya.

1. Introduction

Landslides and related mass movements are some of the most destructive natural hazards around the world. There are natural as well as man-made causes for the occurrence of landslides in an area. With ever-increasing population and infrastructure development in the mountainous terrain, the area becomes susceptible to landslides and fails subsequently. Global landslide database indicates that worldwide during the period between January 1995 and December 2014, 3876 landslides caused a total of 163,658 deaths and 11,689 injuries (Haque *et al.* 2019). It has been reported that the majority of human lives are lost in the Himalayan region and China (Petley 2012).

There are eleven states and two union territories in the Indian Himalayan region, and of these, the state of Uttarakhand is one of the most susceptible to landslides owing to its peculiar geological and geomorphological conditions. Most of the landslides in the region are triggered during or immediately after the monsoon season, i.e., between June and September (Gupta and Bist 2004; Gupta *et al.* 2016) and also during the extreme climatic conditions observed during recent years. For example, extreme climatic conditions during June 2013 had triggered numerous landslides in the entire state of Uttarakhand destroying more than 250 villages and killing $\sim$6000 people (Martha *et al.* 2015). Besides, there are many chronic landslides all along the river valleys and the hilly townships that are posing a serious threat

to the people and the environment in the region. Some of the chronic landslides in the area are the Wariya landslide (Yamuna valley), Varunavat Parvat landslide and Natela landslide (Bhagirathi valley), Kaliayasaur landslide (Alaknanda valley), Byung Gad landslide (Mandakini valley), Malpa landslide and Khotila landslide (Kali valley), Surabhi Resort landslides (Mussoorie township), Balia Nala landslide and Sher ka Danda landslide (Nainital township), and there are many more including the Totaghati landslide. All these landslides have been studied in isolation by various workers to understand their causes and consequences in the region and on the environment (Sati *et al.* 1998; Gupta and Bist 2004; Chaudhary *et al.* 2010; Onagh *et al.* 2012; Gupta *et al.* 2016, 2017; Jamir *et al.* 2018, 2020; Kundu and Patel 2019; Solanki *et al.* 2019; Ram *et al.* 2020).

Landslide susceptibility is the probability of occurrence of landslides in an area based on local terrain conditions (Brabb 1984). It is the degree to which terrain can be affected by slope movement. To assess the landslide susceptibility in a region, it is important to assess the spatial distribution of the landslides and their controlling factors. The relative weightage to each landslide controlling factor is determined using appropriate models and finally, the landslide susceptibility map is prepared. In recent times, there are a large number of models for the preparation of the landslide susceptibility map (LSM), and depending on the availability of the data and the aerial coverage, it is necessary to select the type of models for their preparation. However, these days with the availability of advanced geographical information system (GIS) technology, it has become easier to carry out the analysis in a shorter time. In general, there are two available methods, qualitative and quantitative for the assessment and preparation of LSMs. The qualitative method is mainly based on the geomorphological analysis and involves assigning weightage to each controlling factor of landslides based on the expert's knowledge and experience. This method is easy to apply but its dependence on the subjectivity of expert opinion is a major limitation as the results may vary depending on the expert's opinion. To overcome this limitation, quantitative methods are used. These methods use statistical techniques based on mathematical relations between landslides and independent landslide-controlling factors. These statistical methods have been widely used during recent years across the world, including the Himalayan region (Gupta and Joshi 1990; Carrara *et al.* 1991; Lee 2005; Mathew *et al.* 2009; Chauhan *et al.* 2010; Kumar and Anbalagan 2015; Ram *et al.* 2020).

There are both qualitative as well as quantitative methods for the landslide susceptibility assessment of an area. In the qualitative methods, relative weights to the various classes of the causative factors of landslides are assigned by the experts on the basis of their knowledge of the subject and the study area, thus the qualitative methods are subjective as the weightage assigned to a particular class of the causative factor might vary from one expert to another (Abella and Weste 2008). In order to overcome this limitation, quantitative methods are widely being used (Guzzetti et al. 1999; Sarkar *et al.* 2013; Kumar and Gupta 2021; Ram and Gupta 2021). In these methods, the spatial distribution of landslides is statistically correlated with various classes of each causative factor of landslides. Broadly, the quantitative methods are deterministic and statistical. Deterministic methods use algorithms that include geotechnical properties of the soil and rocks on the slopes and topographic parameters of slope surfaces and thus are mainly used for very site-specific studies (Solanki *et al.* 2019; Pradhan and Siddique 2020; Kumar *et al.* 2021; Tandon *et al.* 2021). Statistical methods elucidate the correlation between the distribution of landslides and different classes of the causative factors of landslides. Accordingly, the relative weights are assigned. These are bivariate and multivariate. In the bivariate method, the simple relation between the landslide distribution and the causative factor is identified using different statistical methods like Yule's coefficient, frequency ratio, information value and weight of evidence (Fleiss 1991; Agterberg Bonham-Carter *et al.* 1993; Ozdemir and Altural 2013; Ram and Gupta 2021), whereas the multivariate analysis not only encompasses the relationship between the landslide distribution and different causative factors, but also among different causative factors using different techniques like artificial neural networks, logistic regression, random forest, support vector machine, etc. (Sevgen *et al.* 2019; Yu and Chen 2020; Kumar and Gupta 2021). These have been reviewed by Lee (2019) and Shano *et al.* (2020).

Bivariate techniques are widely used for regional-scale landslide susceptibility mapping, as these are easy to use, less time-consuming (Guzzetti *et al.* 1999; Sarkar *et al.* 2013; Kumar and Gupta 2021). Ram and Gupta (2021) explained that all the

bivariate methods exhibit more or less similar success and prediction, nevertheless, the accuracy of the model greatly depends on the various terrain parameters. However, in some particular areas, weight of evidence and information value methods have exhibited higher validation than other methods. The multivariate methods may have higher accuracy than the bivariate methods, however, these are time-consuming and are therefore used for local or small areas. Therefore, in the present study, we have utilized weight of evidence and information value methods as these are easy to use for the larger area.

In the present study, regional-scale landslide susceptibility mapping for the state of Uttarakhand has been carried out using two bivariate methods, the weight of evidence (WoE) and information value (IV). Both these methods are relatively simple to use and have been used widely across the globe and in the Himalayas (Corsini *et al.* 2009; Guri and Patel 2015; Chen *et al.* 2016; Sharma and Mahajan 2019; Cao *et al.* 2021). However, for the first time, the entire state of Uttarakhand is mapped for landslide susceptibility using quantitative techniques, though NRSA (2001), DST (2011) and DMMC (https://dmmc.uk.gov.in/pages/display/96-landslide-zone) have mapped few of the major river corridors of the state of Uttarakhand and Himachal Pradesh using qualitative techniques. The present study will provide first-hand information to the planners as there are lot of activities undergoing in the form of construction and widening of roads, tunnels, bridges, dams, and hydropower, and many are in the developmental stage, despite the growing number and frequency of the landslides in the region.

2. Study area

The study area is in the administrative boundary of the state of Uttarakhand, one of the 13 Indian states located in the Indian Himalayan region (IHR). It is located in the northwest Himalaya between longitude 77°33′44″–81°01′10″ E and latitude 28°42′58″–31°28′20″N (figure 1). It covers an area of ∼53,483 km². It is also known as Devbhoomi as it houses four famous pilgrimage shrines, Yamunotri, Gangotri, Kedarnath, and Badrinath. The area is traversed by N–S trending major rivers like Yamuna, Bhagirathi, Alaknanda, and Kali originating from the Yamunotri, Gangotri, Satopanth, and Kalapaani glaciers, respectively.

Geologically, the study area comprises all the tectonic divisions of the Himalaya and these from south to north are sediments of the Indo-Gangetic plains, Outer Himalaya, Lesser Himalaya, Higher Himalaya, and Trans-Himalaya (Thakur 1992). Outer Himalaya, also known as Siwalik Group, is bounded by the Himalayan Frontal Thrust (HFT) in the south and Main Boundary Thrust (MBT) in the north. It mainly consists of sandstones with alteration with clays and claystone and conglomerates. The Lesser Himalaya lies between the Main Boundary Thrust (MBT) and the Main Central Thrust (MCT). It includes sedimentary and meta-sedimentary rocks. These rocks are categorized under different groups and formations, like Beringa Formation, Damta Group (Chakrata and Rautgara formations), Tejam Group (Deoban and Mandhali formations), and Chandpur, Nagthat, Blaini, Infra-Krol, Krol, and Tal formations. However, the dominant rock types constituting the Lesser Himalayan rocks are quartzite, greywacke, siltstone, slate, limestone/dolomite, granite, phyllite, and schist. The Higher Himalaya, a thick crystalline zones, mainly constituting metamorphic schists and gneisses, is sandwiched between MCT in the south and the South Tibetan Detachment in the north. These rocks have also been referred to as central crystallines (Heim and Gansser 1939). Trans-Himalaya or Tethys Himalaya lies above the Higher Himalaya and consists mainly of granite and varying rocks belonging to the Tethyan sequences.

Geomorphologically, the northern part of the area is marked by deep gorges, glaciated valleys, steep to very steep slopes, and high relief with triangular facets, whereas the southern part of the area has wider valleys with point bar deposits and fluvial terraces. The elevation, in general, gradually increases from south to north of the study area and in the vicinity of the MCT, there is a steep rise in elevation of the area. The relief of the area is 7654 m with elevations varying between 123 and 7777 m.

The area is under the influence of monsoon rainfall, falling mostly in the months between June and September every year. The area in the vicinity of the MCT acts as an orographic barrier, therefore the area north of MCT receives a sustained amount of liquid precipitation in the valleys and slopes that are below 3 km. The precipitation in the area is highly variable, the average annual rainfall is ∼2000 mm with > 80% recorded during the monsoon season. The area had also witnessed few climatic extreme events in the form of concentrated rainfall at few places leading to slope failures (Martha *et al.* 2015; Kumari *et al.* 2019).
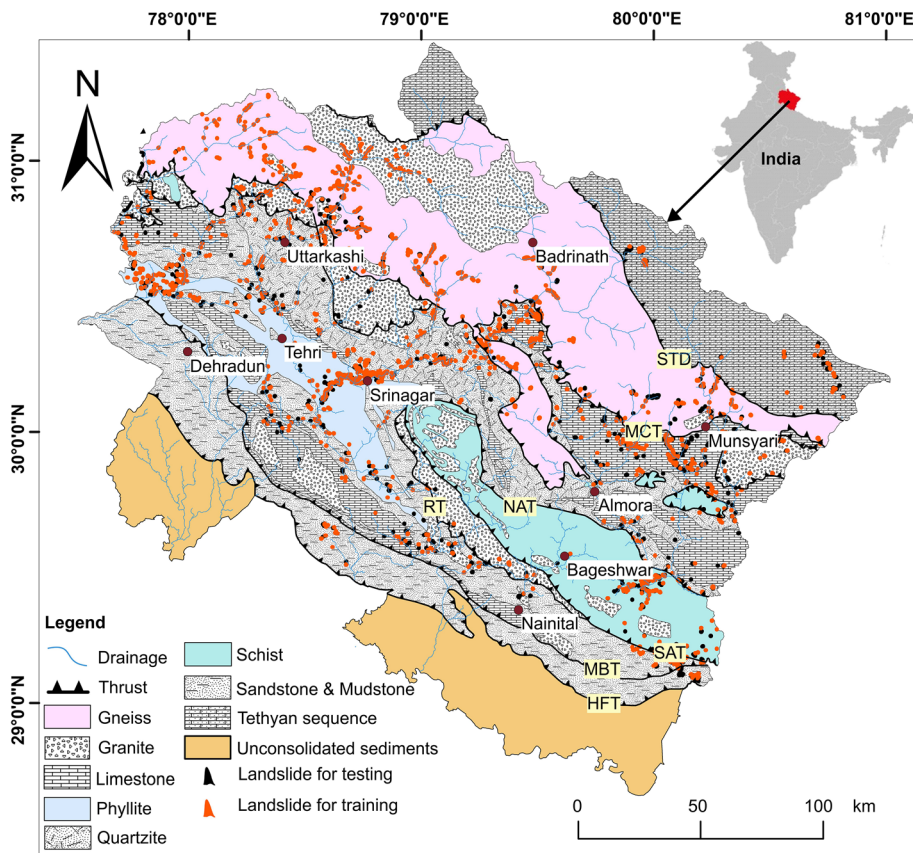
Figure 1. Location map of the area depicting the spatial distribution of major lithounits as well the landslides (HFT: Himalayan Frontal Thrust, MBT: Main Boundary Thrust, RT: Rautgaura Thrust, SAT: South Almora Thrust, NAT: North Almora Thrust, MCT: Main Central Thrust and STD: South Tibetan Detachment).

3. Data used and methodology

Data used for the present study were extracted from high-resolution satellite images (IRS-P5 Cartosat-1, Resourcesat-1 multispectral LISS IV and Landsat-8) and high-resolution satellite images on Google Earth platform. Extensive field surveys, particularly along the road tracks and river valleys have also been undertaken. The characteristic features of the satellite images used in the present study are listed in table 1.

The regional-scale landslide susceptibility mapping involves: (i) cataloging of the spatial distribution of active landslides in the area, (ii) identifying and preparation of thematic maps involving the controlling factors of landslides, (iii) selection of data for the training and validation of the models, (iv) calculating the weightage to each class of landslide controlling factor by applying the bivariate weight of evidence (WoE) and the information value (IV) models, (v) constructing landslide susceptibility maps, and finally (vi) the performance and the validation of the models. These are briefly described hereunder:

3.1 *Cataloging of the spatial distribution of active landslides*

The identification of the spatial distribution of landslide in the area is one of the prerequisites for any kind of study involving landslide hazard and susceptibility in a large area (Carrara *et al.* 1995; Champatiray 1996; Guzzetti *et al.* 1999, 2005; van Westen *et al.* 2008) as it has been hypothesized that previous history of landslides in an area dictates the future distribution of landslides under similar influencing factors. Therefore, landslide inventory was prepared using satellite images and extensive field survey in the area.

3.2 *Identifying and preparation of the thematic maps of the controlling factors of landslides*

Eleven possible controlling factors of landslides were considered. These are lithology, elevation, degree of slope and slope aspect, plan and profile curvature, distance to thrust, road and drainage, topographic wetness index, and the land-use type. Lithology plays an important role in the

Table 1. *The characteristic features of the satellite images used for the present study.*

Satellite data	Source	Spatial resolution (m)	Date
IRS P-5	Cartosat-1	2.5	2014–2017
Resourcesat-2	LISS IV	5.8	03 November 2013
			01 December 2013
Google Earth Imagery	CNES/Airbus and Digital Globe, Bird views	1.0–1.5	2015–2019
Landsat-8	OLI/TIRS	30	2019, 2020

distribution of landslides in an area as different lithological units have different geotechnical and hydrogeological properties that control the stability of the slope and the distribution of landslides. Therefore, a lithological map of the region was prepared by digitizing the lithological units from a geological map of the area (Thakur 1992).

The topography of the terrain, in general, control the distribution of landslides, therefore various terrain topographic parameters like elevation, degree of slope, slope aspects, plan and profile curvatures, and topographic wetness index were taken into consideration and were extracted from the DEM of the area that was prepared with SRTM data having 30-m spatial resolution. Linear features, like thrust and fault, road, and drainage network weaken the rock mass in its proximity and thus affect the slope stability. Therefore various buffer zones along these were also taken into consideration. Thrust and fault map was extracted from the published secondary data (Thakur 1992), and the road and drainage network was extracted from Survey of India toposheets and DEM of the area, respectively. The stability of the slope is also controlled by the hydrological characteristics and the land-use pattern of the slope, which are represented by the topographic wetness index (TWI) and the normalized difference vegetation index (NDVI), respectively. These indices are calculated using the following algorithms:

$$TWI = \ln\left(\frac{a}{\tan b}\right)$$

where a is the specific catchment area and b is the gradient of slope.

$$NDVI = \frac{NIR - RED}{NIR + RED}$$

where NIR is the reflection in the near-infrared spectrum, and RED is the reflection in the red range of the spectrum.

In the present study, nine different classes of lithology and slope aspects, seven classes of elevation and degree of slope, and five classes of curvatures were taken into consideration. Seven different classes with 50 m buffer zones around drainage and roads, eight classes with 100 m buffer zones around thrust, four different classes of TWI, and three classes of land use in the area were considered. River Tool, Leica Photogrammetry Suite (LPS) tools of ERDAS imagine 9.2 and Arc-GIS 10.5 software were used for satellite image processing, GIS database generation, analysis, and presentation of final output maps. The flowchart for the methodology used in the present study is presented in figure 2.

3.3 *Selection of data for the training and validation of the models*

To build WoE and IV models and then to validate them, the landslide database was partitioned into two subsets: training and validation subsets. In the present study, 70% of the total landslides are randomly selected for building the models, and the remaining 30% for the prediction capability of the models.

3.4 *Calculating the weightage to each class of the landslide controlling factor*

In the various bivariate statistical models, the relative weightage to each class of landslide controlling factor was determined with the aim that the degree of influence that each landslide controlling factor had, the same degree of influence it would have in the future. In the present case, two different approaches, namely the weight of evidence (WoE) and information value (IV) were used for the calculation of relative weightage of each landslide controlling factor. These two models are briefly described hereunder:

3.4.1 *Weight of evidence*

The weight of evidence (WoE) model is based on the concept of Bayer's theorem that the prior
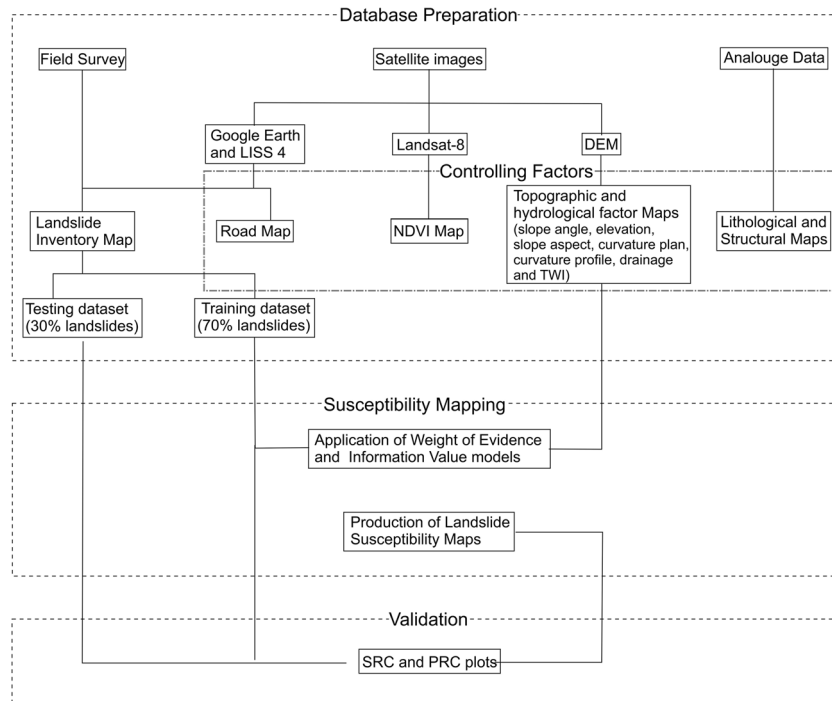
Figure 2. Flowchart used for the preparation of landslide susceptibility maps of the area.

probability of landslides in an area is used to estimate the subsequent probability of landslides in that particular area (Bonham-Carter 1994). In order to assess the strength of each class of controlling factor of landslide, these factors are cross-tabulated with the landslide inventory of the training dataset separately to calculate the positive (W^+) and the negative (W^-) weights using the following equations.

$$W^+ = \ln\left(\frac{A/(A+B)}{C/(C+D)}\right)$$

$$W^- = \ln\left(\frac{B/(A+B)}{D/(C+D)}\right)$$

where A represents the area where a controlling factor and a landslide both are present; B represents the area where landslide is present but controlling factor is absent; C represents the area where controlling factor is present but landslide is absent and D represents the area where a landslide and controlling factor both are absent.

When the controlling factors exhibit a positive relationship with landslides, the W^+ has a positive value and the W^- has a negative value, but when the controlling factors have negative association with landslides, W^+ and W^- indicate negative and positive values, respectively. When the controlling factors have no relationship with the landslides, W^+ and W^- exhibit zero value. The difference

between W^+ and W^- determines the overall relationship of landslides with their controlling factors and is known as weight contrast (C). On the basis of the weight contrast of the various controlling factors of landslides, the final landslide susceptibility map has been prepared.

3.5 *Information value*

The information value (IV) method, a bivariate statistical method, was originally developed by Yin and Yan (1988). It is frequently being used in various geological hazard studies, including landslide susceptibility studies (Chen *et al.* 2016; Sharma and Mahajan 2019). It exhibits the probability of occurrence of the landslide in a particular class of the controlling factor, and is calculated using the following formula:

$$IV_x = \ln\frac{L_x/N_x}{L/N}$$

where IV_x is the information value of class x, L_x is the number of landslide pixels/area in that particular class x, N_x is the total number of pixels/area of class x, L is the total number of landslide pixels/area in the area of study and N is the total number of pixels/area of the entire area of study.

A positive value of IV_x indicates that a particular controlling factor influences the development of

landslides, whereas a negative value indicates that the controlling factor does not have any influence on the development of landslides. Further, the higher the value of IV_x, the stronger is the relationship between the two.

3.6 *Constructing landslide susceptibility maps*

In order to prepare the landslide susceptibility maps using WoE and IV methods, the landslide susceptibility index (LSI) for both the methods was calculated by the summation of weighted values of all the possible classes within that controlling factor, i.e., $LSI = \sum_{x_{i=1}}^{n} C_x$ for the WoE and $LSI = \sum_{x_{i=1}}^{n} IV_x$ for the IV.

LSI indicates the probability of occurrence of landslide for a particular area in the entire study area. The higher the LSI, the higher is the probability of occurrence of a landslide in a particular area. LSIs were classified utilizing natural break classifier into five ordinal zones of landslide susceptibility depicting very high, high, medium, low, and very low landslide susceptibility zones.

3.7 *Performance and the validation of the models*

The performance of both the models used for preparation of landslide susceptibility maps was evaluated by comparing the number of landslide incidences of the validation datasets that were correctly classified against the landslide incidences that were misclassified in the model. This was visualized in a 'success rate curve' (SRC) (Chung and Fabbri 1999; Guzzetti *et al.* 2006). The SRC shows how many landslides in the trailing dataset are successfully captured in the susceptibility map and represents the model efficacy. Further, to estimate the unknown future landslide, a predictive rate curve (PRC) that calculates the percentage of correctly classified landslide incidences in the model has been used.

4. Results

4.1 *Landslide inventory*

An inventory of 3303 active landslides was prepared (figure 1). The area of individual landslides varies between 50 m^2 and 1.5 km^2 and the cumulative area coverage of landslides is ∼ 64 km^2 which is ∼ 0.12% of the study area. In the present study, for both the models, 2312 landslides were randomly selected for building the models, and the remaining 991 landslides were used for the prediction capability of the models.

4.2 *Landslide controlling factors and their relationship with the landslides*

The eleven thematic maps of the controlling factors of landslides (figure 3a–j), including the lithology map (figure 1) were prepared and the strength of the relationship for each class of eleven landslide controlling factors and the occurrences of landslides for both the models, i.e., C for the weight of evidence and IV for the information value methods were calculated and are presented in table 2, and are briefly described hereunder.

4.2.1 *Weight of evidence method*

Among all the lithologies present in the study area, limestone is observed to exhibit the highest strength of relationship with landslides with a C value of 0.78, followed by gneiss, quartzite, and phyllite with C values of 0.69, 0.58, and 0.48, respectively, while the schist, sandstone/mudstone, and granite along with the sediments of the Tethyan sequence and the Gangetic plains indicate the negative correlation. Elevation class ranging between 2001–3000 m and 3001–4000 m exhibit the highest strength of relationship having C value of 0.85 and 0.84, respectively, followed by class 1001–2000 with C value of 0.15, whereas the elevation class > 4001 m and < 1000 m indicate the negative association with landslides. Among different slope classes, 51°–60° slope class indicates the highest strength of relationship with C value of 0.93 followed by 41°–50° slope class and > 60° slope class having C values of 0.78 and 0.75, respectively. Slope class 31°–40° indicates low C value of 0.35, whereas < 30° slope class exhibits the negative strength of the relation. The slope directing towards the southeast exhibits the highest strength of relationship with C value of 0.42, followed by the south and southwest classes with C value of 0.40 and 0.24, respectively, whereas all other slope directions indicate negative association with the landslide, and the flat surface indicate no association with landslides. Also, the concave surfaces and highly convex surfaces for the plan curvature and the highly concave and highly convex surfaces for the profile curvature indicate a strong correlation with landslides, whereas the flat slope surfaces and
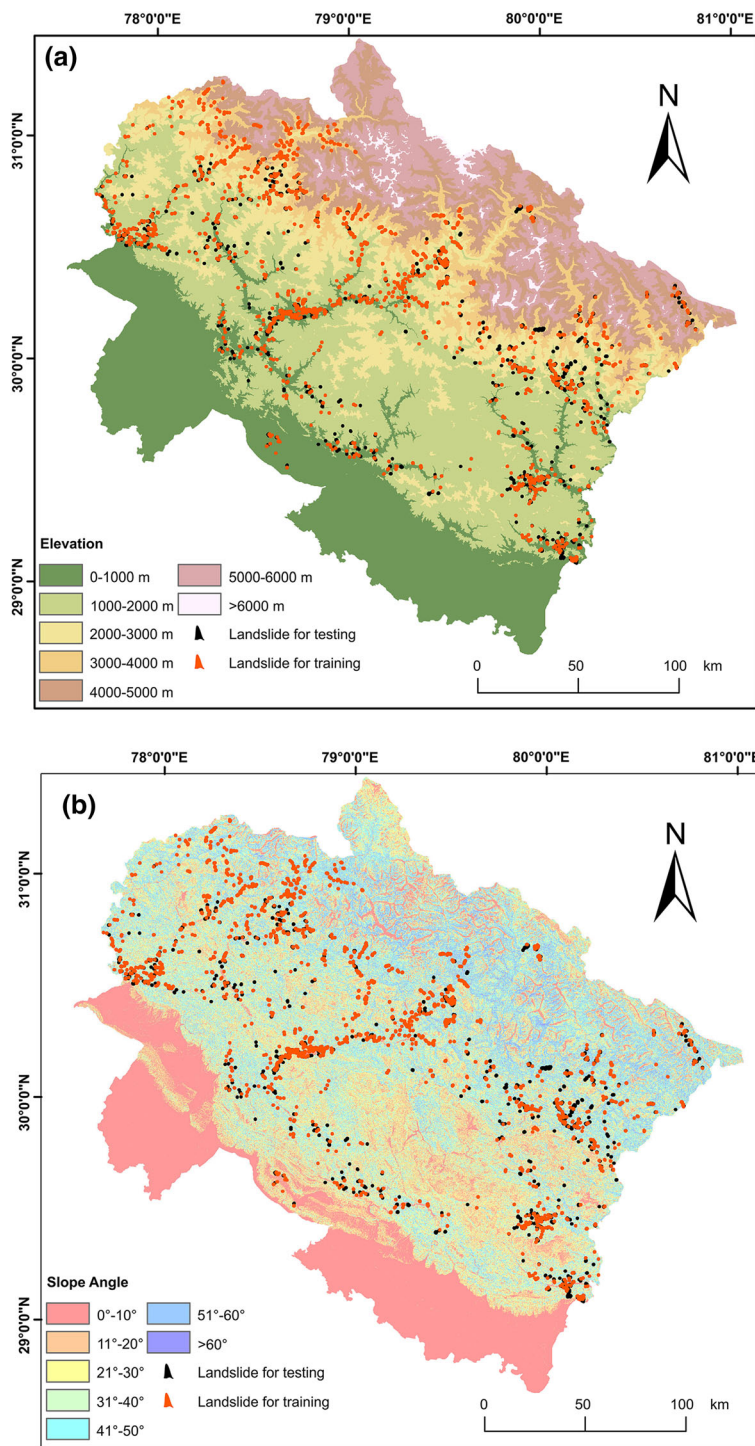
Figure 3. The thematic maps of the controlling factors of landslides **(a)** elevation, **(b)** degree of slope, **(c)** slope aspect, **(d)** plan curvature, **(e)** profile curvature, **(f)** distance to thrust, **(g)** distance to drainage, **(h)** distance to road, **(i)** topographic wetness index, and **(j)** normalized difference vegetation index.

other surfaces exhibit a negative relationship with the landslides. Further, the proximity of thrust, drainage and road with respect to the distribution of occurrences of landslides in the 100 m buffer zones along thrust, and 50 m buffer zones along drainage and road, indicate that the thrusts do not seem to control the distribution of landslides as the

C exhibit negative values in the vicinity of the thrust, whereas the road and drainage classes in the immediate vicinity indicate higher strength of relation with positive C values, and the strength decreases moving away from these features with some variations. The highest C value for TWI has been observed in classes 5–10 with C value of 0.36,
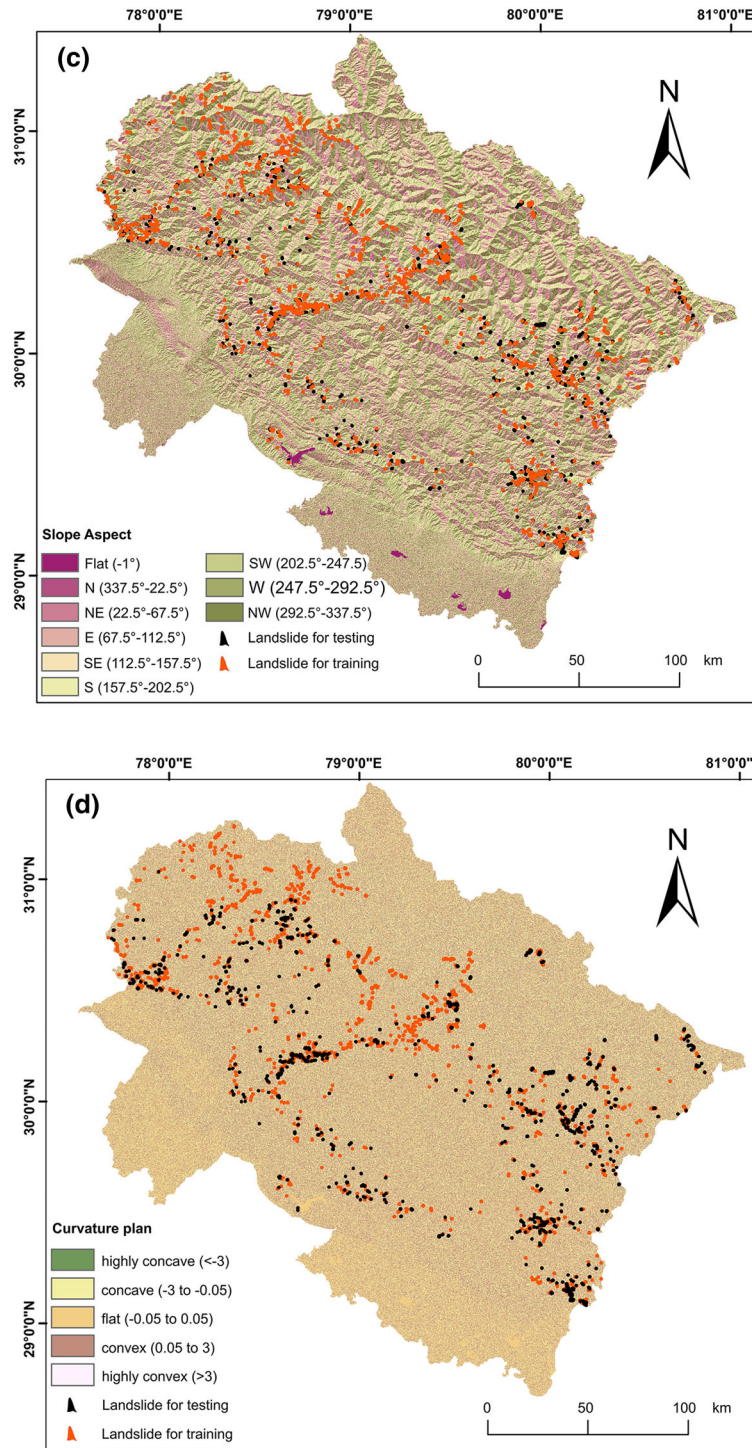
Figure 3. (*Continued.*)

followed by class < 5 (0.29), and classes 11–15 and > 15 indicate a negative association with landslides. NDVI indicates that bare soil exhibits a strong correlation with the occurrence of landslides with C value of 0.69, followed by shrub and grassland with C value of 0.28, and the dense vegetation indicates a negative association.

4.2.2 *Information value method*

Similar to the WoE method, in the IV method also limestone exhibits the highest IV of 0.66, followed by quartzite (0.51), gneiss (0.50), and phyllite (0.45), whereas other litho-units either indicate negative IV or zero value. The elevation classes 2001–4000 m exhibit the higher IV value, whereas all other
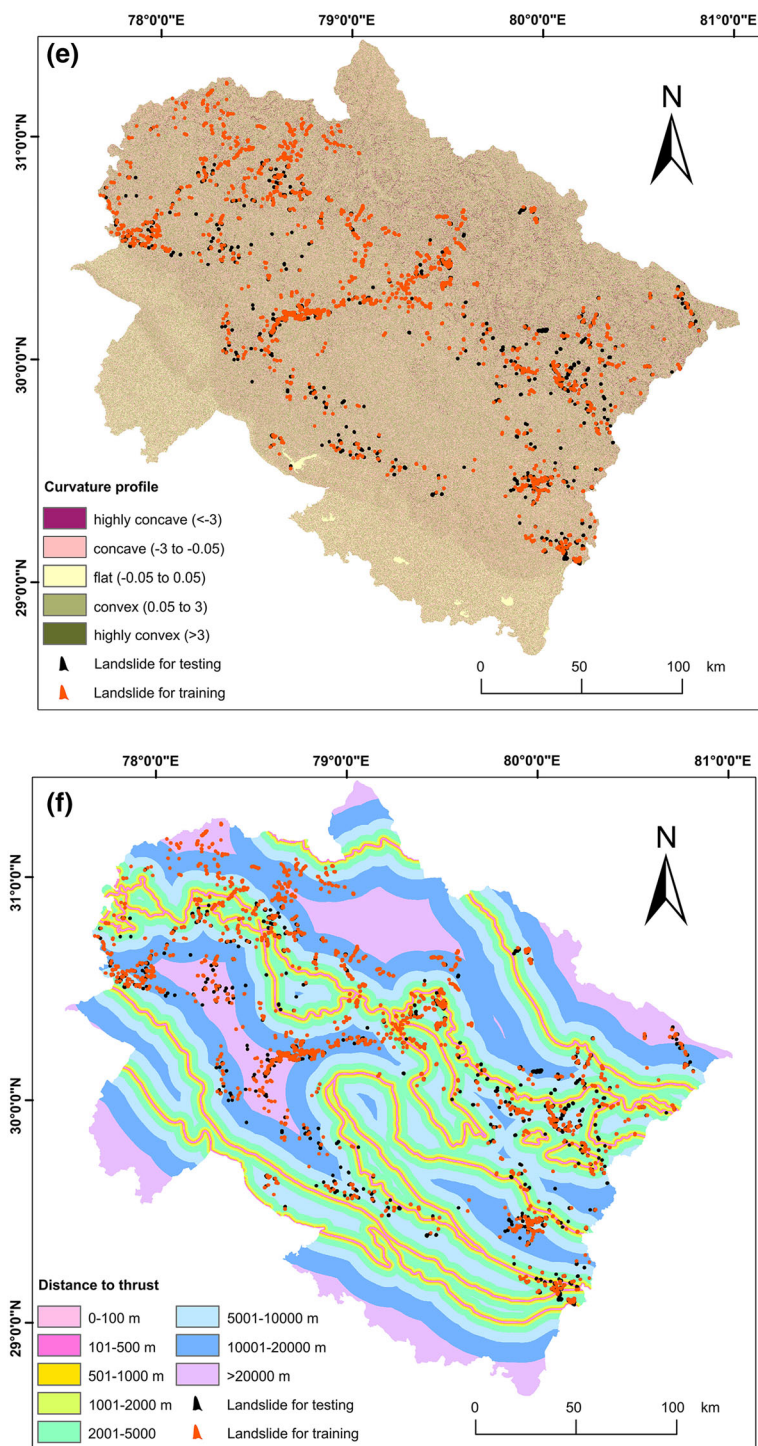
Figure 3. (*Continued.*)

elevation range either indicate weak association or no association at all with landslides. Similar to the WoE method, the slope angle classes 51°–60°, > 60°, and 41°–50° exhibit higher positive association with landslide having IV value of 0.75, 0.74, and 0.62, respectively, whereas weak positive association of landslides is exhibited in 31°–40° slope class, and all the slope class < 30° indicate negative association

with the landslide occurrence. All the south-directing slope classes exhibit positive IV value, while the flat surface and north-facing slopes show a zero or negative relation with the landslide occurrences in the area. Strong and positive relation has been observed for concave and highly convex slopes for the plan curvature and highly concave and convex slopes for the profile curvature of the slope, respectively,
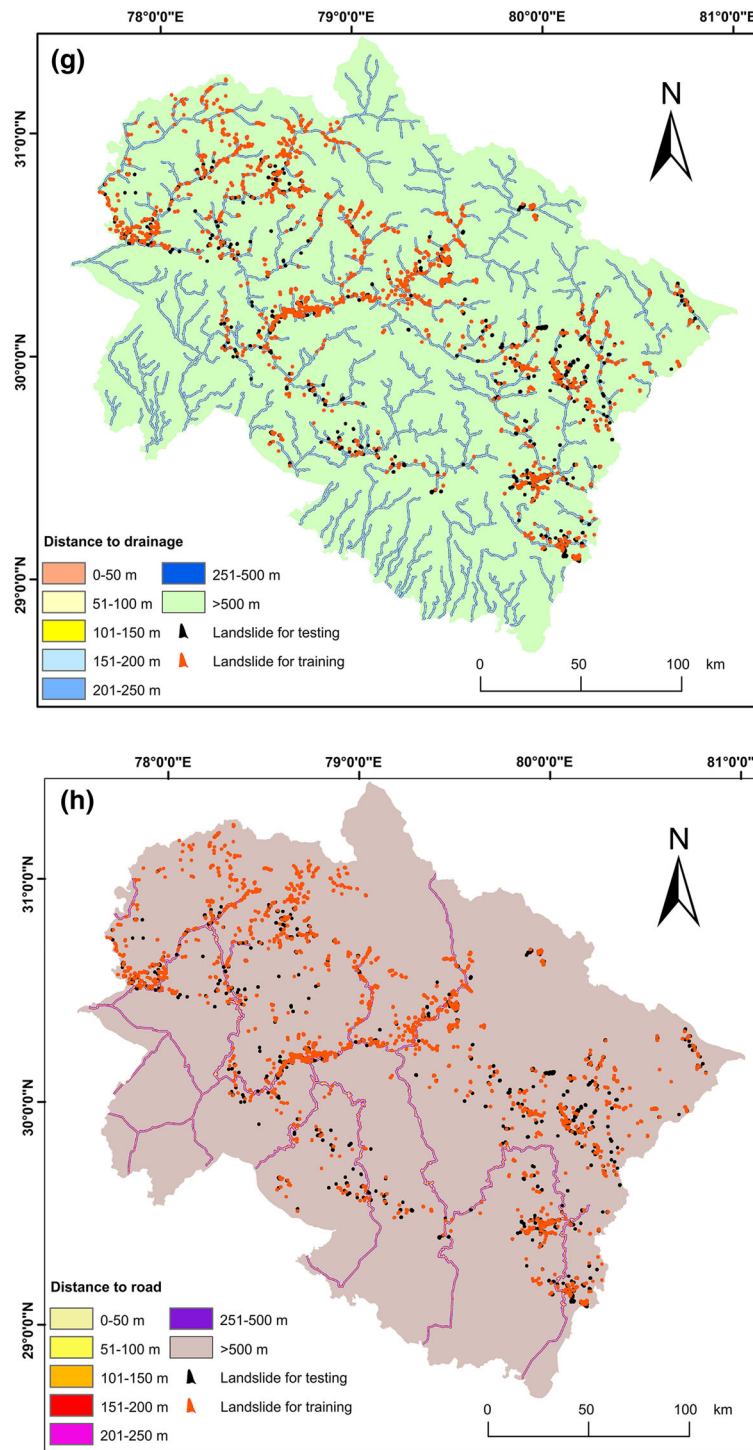
Figure 3. (*Continued.*)

whereas negative relation has been noted for the flat surfaces. Likewise in the WoE method, in the IV method, the proximity of the thrust does not seem to be related to the occurrences of landslides as the IV values in the class nearest to thrust is 0.10, and is maximum in class quite away from the thrust. While the road and drainage network exhibit a strong correlation with the occurrence of landslides as the IV value is maximum in the class proximity to these and is clearly depicted table 2. The topographical wetness index exhibits that class < 5 has the maximum IV value of 0.29, followed by 5–10 class having a value of 0.16, whereas 0–15 and > 15 class do not indicate any relation. While the bare soil class exhibits the highest IV value of 0.37 followed by shrub and grassland class having IV value of 0.21. Dense vegetation class does
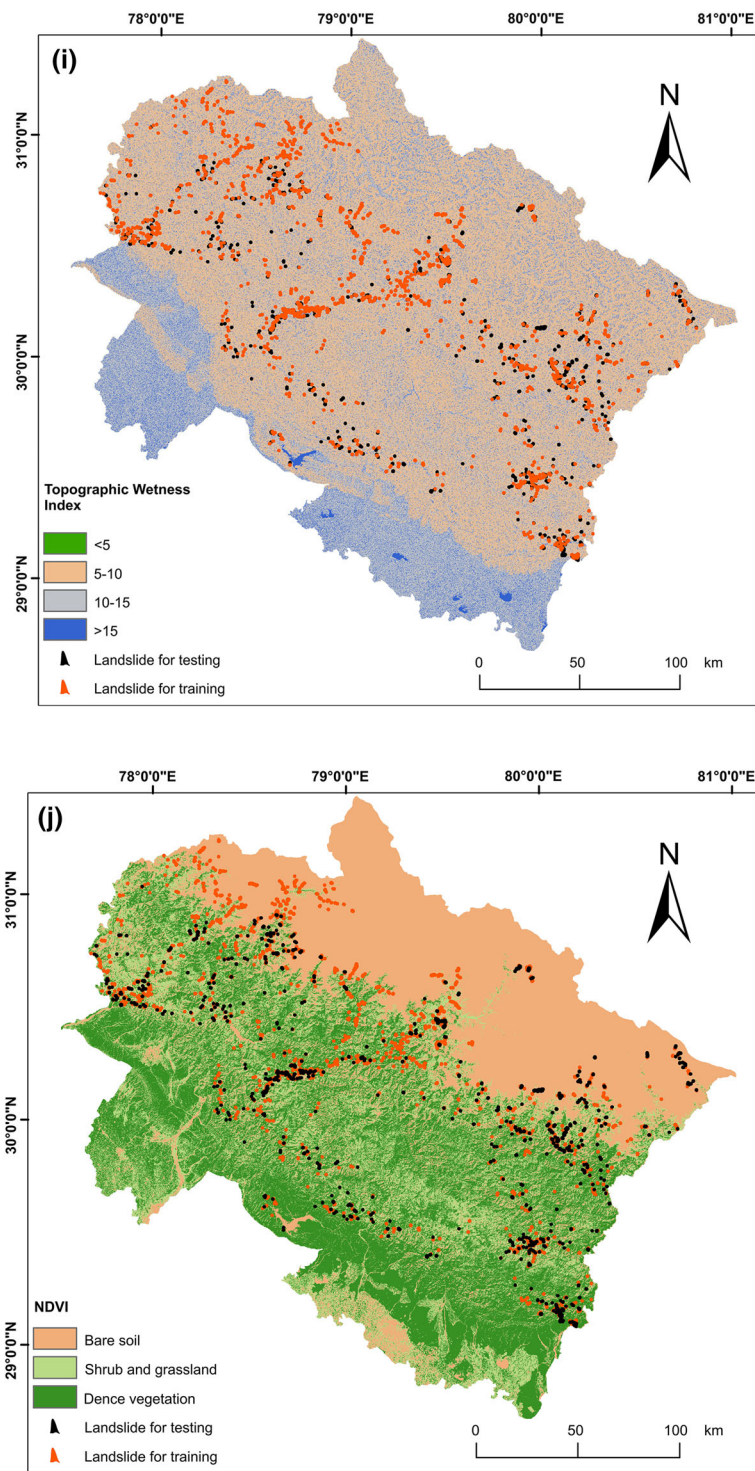
Figure 3. (*Continued.*)

not exhibit any relation with landslides as it has a negative IV value.

4.3 *Landslide susceptibility mapping*

Landslide susceptibility maps depicting five classes of hazards, viz., very low, low, moderate, high and very high hazards, using WoE and IV methods have been prepared and are presented in figure 4(a and b), respectively. It has been observed that LSM prepared by WoE exhibits that 25% and 26% area falls in very low and low susceptible zones, 22% in moderate, and 18% and 9% in high and very high susceptible zones. LSM prepared using IV indicates more or less similar results (figure 5). Further, it has been noted that the major area lying in the high and

Table 2. *The strength of the relationship for each class of 11 landslide controlling factors and the occurrences of landslides for both the weight of evidence and the information value models.*

Controlling factors	Class	N_x (class area) (km^2)	L_x (landslide area) (km^2)	Wi$^+$	Wi$^-$	C	L_x/N_x (landslide density)	IV
Lithology	Granite	6543	4.2	− 0.19	0.02	− 0.21	0.0006	− 0.19
	Phyllite	2324	2.9	0.45	− 0.03	0.48	0.0012	0.45
	Limestone	5589	8.5	0.66	− 0.12	0.78	0.0015	0.66
	Sandstone/mudstone	8460	2.4	− 1.00	0.11	− 1.11	0.0003	− 0.99
	Quartzite	4853	6.3	0.51	− 0.07	0.58	0.0013	0.51
	Tethyan sediments	4851	2.2	− 0.52	0.04	− 0.56	0.0005	− 0.52
	Unconsolidated sediments (Gangetic plain)	6237	0.0	0.00	0.12	− 0.12	0.0000	0.00
	Schist	3643	0.9	− 1.15	0.05	− 1.20	0.0002	− 1.15
	Gneiss	11151	14.4	0.51	− 0.19	0.69	0.0013	0.50
Elevation	< 1000 m	13770	7.6	− 0.34	0.10	− 0.44	0.0006	− 0.34
	1001–2000 m	17503	15.1	0.10	− 0.05	0.15	0.0009	0.10
	2001–3000 m	7124	11.0	0.69	− 0.16	0.85	0.0016	0.68
	3001–4000 m	4122	6.8	0.74	− 0.10	0.84	0.0016	0.74
	4001–5000 m	5812	1.4	− 1.18	0.08	− 1.26	0.0002	− 1.18
	5001–6000 m	4874	0.0	0.00	0.10	− 0.10	0.0000	0.00
	> 6000 m	445	0.0	0.00	0.01	− 0.01	0.0000	0.00
Slope	0°–10°	11398	0.5	− 2.83	0.23	− 3.06	0.0000	− 2.83
	11°–20°	9336	3.3	− 0.79	0.11	− 0.90	0.0004	− 0.79
	21°–30°	9753	6.2	− 0.20	0.04	− 0.24	0.0006	− 0.20
	31°–40°	7781	8.1	0.29	− 0.06	0.35	0.0010	0.29
	41°–50°	8051	11.7	0.62	− 0.16	0.78	0.0014	0.62
	51°–60°	7010	11.6	0.75	− 0.18	0.93	0.0016	0.75
	> 60°	320	0.5	0.74	− 0.01	0.75	0.0016	0.74
Slope aspect	Flat (−1°)	190	0.0	0.00	0.00	0.00	0.0000	0.00
	N (337.5°–22.5°)	6548	3	− 0.55	0.03	− 0.57	0.0005	− 0.55
	NE (22.5°–67.5°)	6311	3.3	− 0.41	0.04	− 0.46	0.0005	− 0.41
	E (67.5°–112.5°)	6300	4.1	− 0.18	0.02	− 0.20	0.0007	− 0.18
	SE (112.5°–157.5°)	6924	7.7	0.35	− 0.07	0.42	0.0011	0.35
	S (157.5°–202.5°)	7144	7.8	0.33	− 0.06	0.40	0.0011	0.33
	SW (202.5°–247.5°)	7441	7.1	0.20	− 0.04	0.24	0.0010	0.20
	W (247.5°–292.5°)	6596	4.9	− 0.04	0.01	− 0.05	0.0007	− 0.04
	NW (292.5°–337.5°)	6198	4.0	− 0.19	0.02	− 0.21	0.0006	− 0.19
Plan curvature	Highly concave (< −3)	414	0.6	0.70	− 0.01	0.70	0.0016	0.69
	Concave (−3 to −0.05)	23376	20.9	0.13	− 0.12	0.25	0.0009	0.13
	Flat (−0.05 to 0.05)	5756	2.2	− 0.72	0.06	− 0.78	0.0004	− 0.72
	Convex (0.05 to 3)	23654	17.7	− 0.05	0.04	− 0.08	0.0007	− 0.05
	Highly convex (> 3)	450	0.6	0.47	− 0.01	0.47	0.0012	0.47
Profile curvature	Highly concave (< −3)	829	1.1	0.51	− 0.01	0.52	0.0013	0.51
	Concave (−3 to −0.05)	23197	17.4	− 0.04	0.03	− 0.07	0.0008	− 0.04
	Flat (−0.05 to 0.05)	4841	1.9	− 0.70	0.05	− 0.75	0.0004	− 0.70
	Convex (0.05 to 3)	23946	20.2	0.07	− 0.06	0.14	0.0008	0.07
	Highly convex (> 3)	837	1.4	0.76	− 0.02	0.78	0.0017	0.76

Table 2. *(Continued.)*

Controlling factors	Class	N_x (class area) (km^2)	L_x (landslide area) (km^2)	Wi$^+$	Wi$^-$	C	L_x/N_x (landslide density)	IV
Drainage	0–50 m	678	2.4	1.49	− 0.05	1.54	0.0035	1.49
	51–100 m	671	3.2	1.83	− 0.07	1.90	0.0048	1.82
	101–150 m	658	3.1	1.79	− 0.06	1.86	0.0047	1.79
	151–200 m	647	2.4	1.58	− 0.05	1.62	0.0038	1.57
	201–250 m	639	1.9	1.33	− 0.03	1.37	0.0030	1.33
	251–500 m	3179	5.8	0.85	− 0.09	0.94	0.0018	0.85
	> 500 m	47179	23.1	− 0.47	1.32	− 1.79	0.0005	− 0.47
Thrust	0–100 m	508	0.2	− 0.61	0.00	− 0.61	0.0004	− 0.61
	101–500 m	1885	1.2	− 0.21	0.01	− 0.21	0.0006	− 0.21
	501–1000 m	2330	1.6	− 0.14	0.01	− 0.14	0.0007	− 0.14
	1001–2000 m	4404	3.7	0.06	− 0.01	0.07	0.0008	0.06
	2001–5000 m	11168	8.6	− 0.01	0.00	− 0.02	0.0008	− 0.01
	5001–10,000 m	12377	11.7	0.19	− 0.07	0.26	0.0009	0.19
	10,001–20,000 m	14058	12.2	0.10	− 0.04	0.14	0.0009	0.10
	> 20,000 m	6921	2.7	− 0.69	0.07	− 0.76	0.0004	− 0.69
Road	0–50 m	212	1.5	2.22	− 0.03	2.26	0.0072	2.22
	51–100 m	184	0.8	1.77	− 0.02	1.79	0.0046	1.77
	101–150 m	178	0.5	1.28	− 0.01	1.29	0.0028	1.28
	151–200 m	125	0.3	1.02	0.00	1.03	0.0022	1.02
	201–250 m	164	0.4	1.06	− 0.01	1.06	0.0023	1.06
	251–500 m	807	1.5	0.87	− 0.02	0.89	0.0019	0.87
	> 500 m	51981	37.0	− 0.10	1.34	− 1.44	0.0007	− 0.10
TWI	< 5	1	0.0	0.29	0.00	0.29	0.0010	0.29
	5–10	26758	24.6	0.16	− 0.19	0.36	0.0009	0.16
	10–15	21290	13.7	− 0.20	0.11	− 0.31	0.0006	− 0.20
	> 15	5601	3.6	− 0.19	0.02	− 0.21	0.0006	− 0.19
NDVI	Bare soil	20026	22.8	0.37	− 0.31	0.69	0.0011	0.37
	Shrub and grassland	12830	12.3	0.21	− 0.08	0.28	0.0010	0.21
	Dense vegetation	20794	6.9	− 0.86	0.31	− 1.18	0.0003	− 0.86

very high landslide susceptible zones are on the slopes ranging between 40° and 60°, located at an elevation ranging between 2000 and 4000 m and the southern-side directing slopes. These are mainly located in the vicinity of the MCT. The low and very low susceptible zones lie at lower elevations and gentler slopes and occur mainly in the Lesser and Outer Himalaya and in the Indo-Gangetic plains. Some of the religious tourist destinations like Uttarkashi, Badrinath and Munsiayari falls in the high to very high landslide susceptible zones.

4.4 *Anthropogenic intervention of slopes*

Uttarakhand state had its origin in 2000 and since then there is a lot of human interference on slopes in the form of development activities, like construction of hydropower projects, tunnels, dams, bridges, new roads and widening of the existing roads, etc. All these activities require anthropogenic intervention on slopes, in the form of change of geometry of the slopes. Generally, any deviation from the natural angle or the angle of repose of slope may lead to destabilization of slopes, and subsequently, the slopes may either fail instantaneously or in due course of time, if not treated immediately. Due to all these activities, the area has witnessed development of slope instability and landslides at many places. Few recent examples of such failure, triggered by the rainfall, have been witnessed along the road-cut section or widening of roads section on the Rishikesh–Badrinath highway in the Tota Ghati area (https://www.amarujala.com/photo-gallery/dehradun/badrinath-highway-open-after-six-days-in-tota-ghati-but-threat-of-landslide-remains-intact).

The present study using both the models, i.e., weight of evidence and the information value, depicts the positive relation of the spatial distribution of landslides with the distribution of roads and drainage network in the area, and the strength decreases moving away from these features (table 2). It is, therefore, of utmost importance
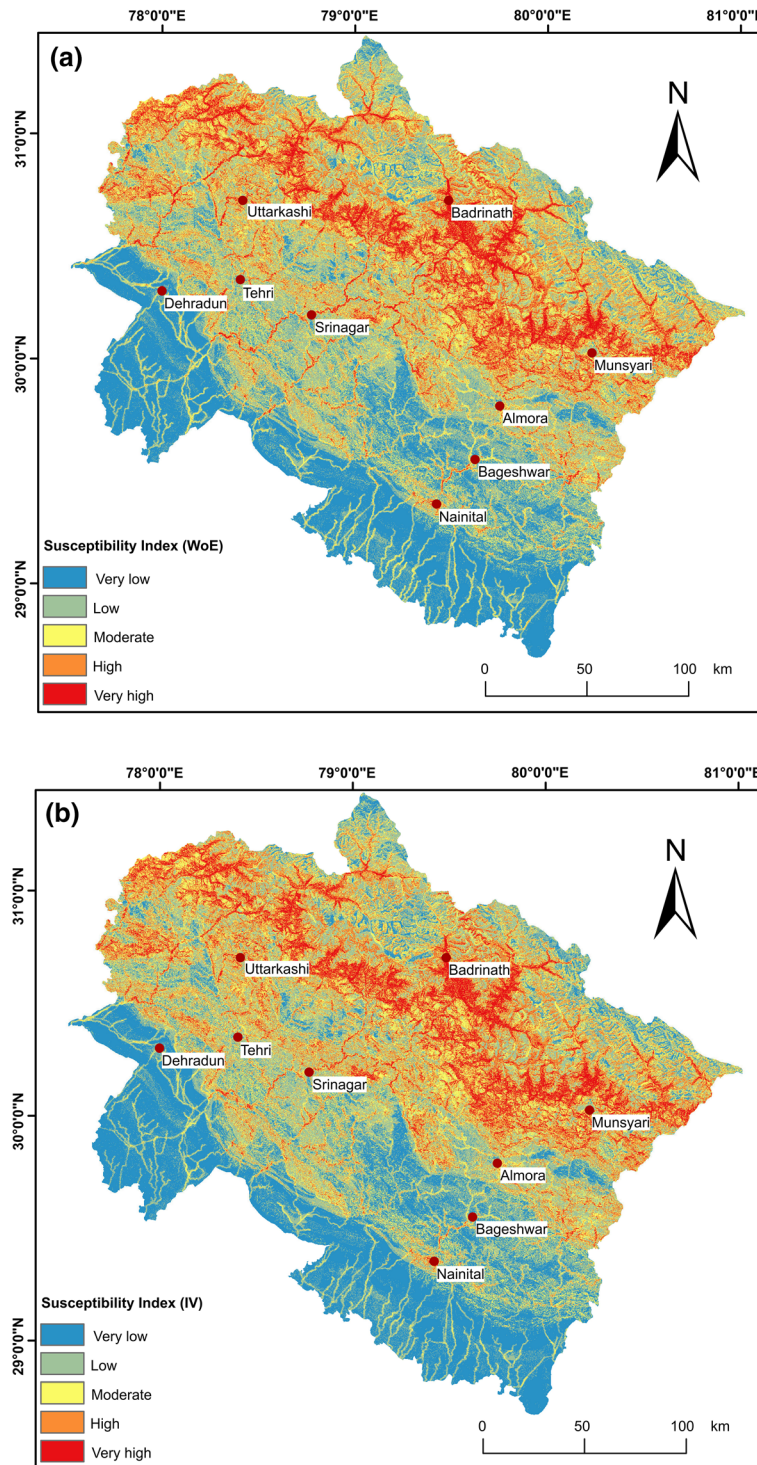
Figure 4. Landslide susceptibility maps depicting very low, low, moderate, high and very high landslide susceptibility zones using **(a)** weight of evidence and **(b)** information value methods.

that any change in the geometry of slope must be evaluated carefully at the local scale, particularly in the high and very high landslide susceptibility zones (figure 4a, b), and the landslide susceptibility maps of the region should be considered for the first-hand information to guide the development activities in the region.

4.5 *Validation of the landslide susceptibility mapping*

The landslide susceptible maps prepared using WoE and IV models are validated by preparing the success rate curve (SRC) and the prediction rate curve (PRC). The SRC plot between cumulative
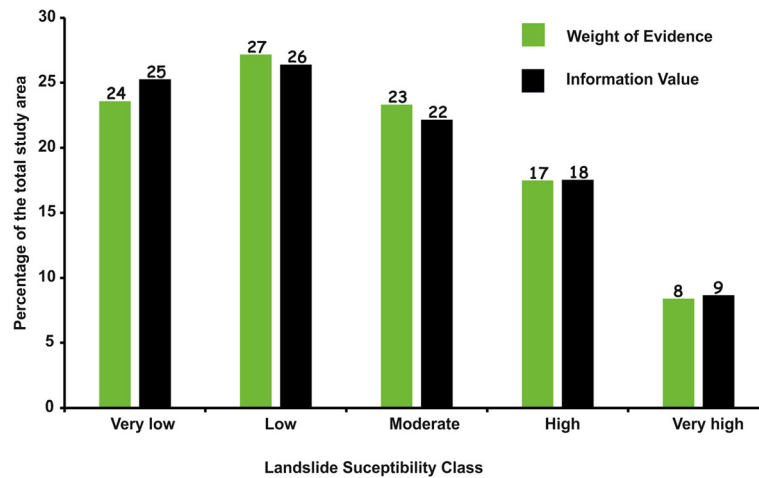
Figure 5. Bar diagram indicating the percentage of areas falling in different landslide susceptibility zones of weight of evidence and information value methods.
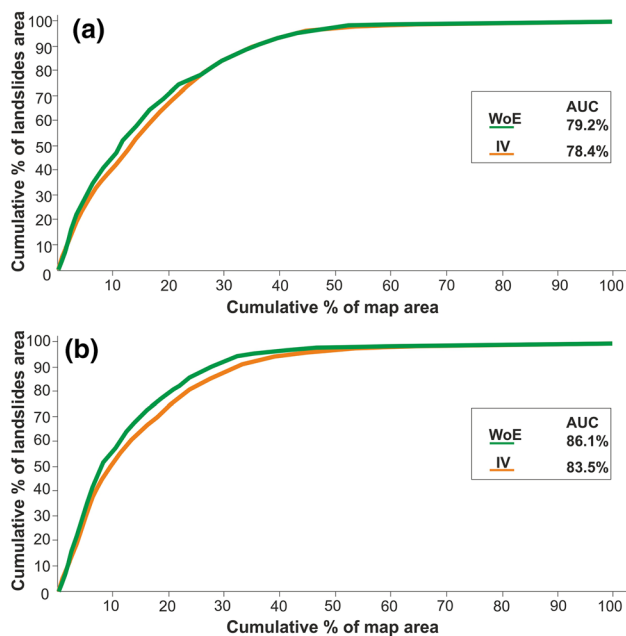

Figure 6. **(a)** Success rate curve (SRC) and **(b)** prediction rate curve (PRC) for the weight of evidence and information value methods.

percent of the training landslides area and the cumulative percent of the susceptible map area (figure 6a) represents the number of landslides successfully captured in the susceptibility map and reflects the efficacy of the model. Whereas PRC plot between cumulative percent of the testing landslides area and the cumulative percent of the susceptible map area (figure 6b) is used to estimate the unknown future landslides and represent the accuracy of classified landslide susceptible maps that have been prepared. It has been noted that the

area under curve (AUC) of SRC is 79.2% and 78.4%, and PRC is 86.1% and 83.5% for the WoE and IV model, respectively, indicating that of the two models, WoE has somewhat better efficacy and accuracy.

5. Conclusions

The present study exhibits the spatial distribution of landslide susceptible zones of the state of Uttarakhand by preparing the landslide susceptible maps using weight of evidence and information value methods. This study concludes that:

- Around 51% of the area is located in the high and very high landslide susceptible zones, 22–23% in the moderate and $\sim$26–27% in the low and very low landslide susceptible zones.
- Both the methods used for the preparation of the landslide susceptible maps indicate more or less similar efficacy and accuracy, though, for the present area of study, WoE model is somewhat better than the IV model.
- In the present day climatic scenario of the state of Uttarakhand, limestone, gneiss, quartzite and phyllite have higher propensity towards the development of landslides.
- Most of the high and very high landslide susceptible zones are located in the vicinity of the Main Central Thrust, and in the Higher Himalaya, whereas low and very low landslide susceptible zones are located in the Indo-Gangetic planes, Outer and Lesser Himalayas.
- Slopes ranging between 40° and 60°, located at an elevation between 2000 and 4000 m and

facing towards southern sides are more susceptible to failure and thus fall in the high and very high susceptible zone.

Acknowledgements

Author statement

V Gupta conceived the idea. V Gupta, S Kumar, R Kaur and R S Tandon helped in data collection. S Kumar, R Kaur analyzed the data. All the authors contributed towards writing the manuscript.

References

Abella E A C and Van Weste C J 2008 Qualitative landslide susceptibility assessment by multicriteria analysis: A case study from San Antonio del Sur, Guantánamo, Cuba; *Geomorphology* **94(3–4)** 453–466.

Agterberg Bonham-Carter G F, Cheng Q M and Wright D F 1993 Weights of evidence modeling and weighted logistic regression for mineral potential mapping; *Comput. Geol.* **25** 13–32.

Bonham-Carter G F 1994 *Geographic information systems for geoscientists – modeling with GIS*; Pergamon Press, 416p.

Brabb E E 1984 Innovative approaches to landslide hazard mapping; *Proc. 4th International Symposium on Landslides*, Toronto **1** 307–324.

Cao Y, Wei X, Fan W, Nan Y, Xiong W and Zhang S 2021 Landslide susceptibility assessment using the weight of evidence method: A case study in Xunyang area, China; *PLoS ONE* **16(1)** e0245668.

Carrara A, Cardinali M, Detti R, Guzzetti F, Pasqui V and Reichenbach P 1991 GIS techniques and statistical models in evaluating landslide hazard; *Earth Surf. Process. Landf.* **16**(5) 427–445.

Carrara A, Cardinali M, Guzzetti F and Reichenbach P 1995 GIS technology in mapping landslide hazard; In: *Geographical Information Systems in assessing natural hazards,* pp. 135–175.

Champatiray P K 1996 Landslide hazard zonation using fuzzy logic and probability analysis in western Himalayas; Project report under IIRS-ITC Programme, Internal Publication, ITC, Netherlands.

Chaudhary S, Gupta V and Sundriyal Y P 2010 Surface and sub-surface characterization of Byung landslide in Mandakini valley, Garhwal Himalaya; *Him. Geol.* **31(2)** 125–132.

Chauhan S, Sharma M and Arora M K 2010 Landslide susceptibility zonation of the Chamoli region, Garhwal Himalayas, using logistic regression model; *Landslides* **7(4)** 411–423.

Chen T, Niu R and Jia X 2016 A comparison of information value and logistic regression models in landslide susceptibility mapping by using GIS; *Environ. Earth Sci.* **75(10)** 867.

Chung C J F and Fabbri A G 1999 Probabilistic prediction models for landslide hazard mapping; *Photogram. Eng. Remote Sens.* **65(12)** 1389–1399.

Corsini A, Cervi F and Ronchetti F 2009 Weight of evidence and artificial neural networks for potential groundwater spring mapping: An application to the Mt. Modino area (Northern Apennines, Italy); *Geomorphology* **111(1–2)** 79–87.

DMMC https://dmmc.uk.gov.in/pages/display/96-landslide-zone.

DST 2011 Landslide Hazard Zonation Atlas; Department of Science and Technology, Govt. of India.

Fleiss J L 1991 *Statistical methods for rates and proportions*; Wiley.

Gupta R P and Joshi B C 1990 Landslide hazard zoning using the GIS approach – a case study from the Ramganga catchment, Himalayas; *Eng. Geol.* **28(1–2)** 119–131.

Gupta V and Bist K S 2004 The 23 September 2003 Varunavat Parvat landslide in Uttarkashi township, Uttaranchal; *Curr. Sci.* **87(11)** 1600–1605.

Gupta V, Bhasin R K, Kaynia A M, Kumar V, Saini A S, Tandon R S and Pabst T 2016 Finite element analysis of failed slope by shear strength reduction technique: A case study for Surabhi Resort Landslide, Mussoorie township, Garhwal Himalaya; *Geomat. Nat. Hazards Risk* **7(5)** 1677–1690.

Gupta V, Tandon R S, Venkateshwarlu B, Bhasin R K and Kaynia A M 2017 Accelerated mass movement activities due to increased rainfall in the Nainital township, Kumaun Lesser Himalaya, India; *Zeitschrift Fur Geomorph.* **61(1)** 29–42.

Guri P K and Patel R C 2015 Spatial prediction of landslide susceptibility in parts of Garhwal Himalaya, India, using the weight of evidence modelling; *Environ. Monit. Assess.* **187(6)** 1–25.

Guzzetti F, Salvati P and Stark C P 2005 Evaluation of risk to the population posed by natural hazards in Italy; In: *Landslide risk management* Hungr O, Fell R, Couture R and Eberhardt E (eds) Taylor & Francis Group, London, pp. 381–389.

Guzzetti F, Carrara A, Cardinali M and Reichenbach P 1999 Landslide hazard evaluation: A review of current techniques and their application in a multi-scale study, Central Italy; *Geomorphology* **31(1–4)** 181–216.

Guzzetti F, Reichenbach P, Ardizzone F, Cardinali M and Galli M 2006 Estimating the quality of landslide susceptibility models; *Geomorphology* **81(1–2)** 166–184.

Haque U, Da Silva P F, Devoli G, Pilz J, Zhao B, Khaloua A, Wilopo W, Andersen P, Lu P, Lee J and Yamamoto T 2019 The human cost of global warming: Deadly landslides and their triggers (1995–2014); *Sci Total Environ.* **682** 673–684.

Heim A and Gansser A 1939 Central Himalayan geological observations of the Swiss expeditions 1936; *Helv. Sci. Nat.* **73(1)** 1–245.

Jamir I, Gupta V, Kumar V and Thong G T 2018 Evaluation of Potential Surface Instability in Kharsali Village, Yamuna Valley, NW Himalaya; *J. Mount. Sci.* **14(8)** 1666–1676.

Jamir I, Gupta V, Thong G T and Kumar V 2020 Litho-tectonic and precipitation implications on landslides, Yamuna valley, NW Himalaya; *Phys. Geogr.* **41(4)** 365–388.

Kumar R and Anbalagan R 2015 Landslide susceptibility zonation in part of Tehri reservoir region using frequency ratio, fuzzy logic and GIS; *J. Earth Syst. Sci.* **124(2)** 431–448.

Kumar S and Gupta V 2021 Evaluation of spatial probability of landslides using bivariate and multivariate approaches in the Goriganga valley, Kumaun Himalaya, India; *Nat. Hazards,* doi: https://doi.org/10.1007/s11069-021-04928-x.

Kumar V, Jamir I, Gupta V and Bhasin R K 2021 Inferring potential landslide damming using slope stability, geomorphic constraints and run-out analysis: Case study from the NW Himalaya; *Earth Surf. Dyn.* **9** 351–377.

Kumari S, Haustein K, Javid H, Burton C, Allen M R, Paltan H, Dadson S and Otto F E 2019 Return period of extreme rainfall substantially decreases under 1.5°C and 2.0°C warming: A case study for Uttarakhand, India; *Environ. Res. Lett.* **14(4)** 044033.

Kundu V and Patel R C 2019 Susceptibility status of landslides in Yamuna valley, Uttarakhand, NW-Himalaya, India; *Him. Geol.* **40(1)** 30–49.

Lee S 2005 Application of logistic regression model and its validation for landslide susceptibility mapping using GIS and remote sensing data; *Int. J. Remote Sens.* **26(7)** 1477–1491.

Lee S 2019 Current and future status of GIS-based landslide susceptibility mapping: A literature review; *Korean J. Remote Sens.* **35(1)** 179–193.

Martha T R, Roy P, Govindharaj K B, Kumar K V, Diwakar P G and Dadhwal V K 2015 Landslides triggered by the June 2013 extreme rainfall event in parts of Uttarakhand state, India; *Landslides* **12(1)** 135–146.

Mathew J, Jha V K and Rawat G S 2009 Landslide susceptibility zonation mapping and its validation in part of Garhwal Lesser Himalaya, India, using binary logistic regression analysis and receiver operating characteristic curve method; *Landslides* **6(1)** 17–26.

NRSA 2001 Atlas - Landslide Hazard Zonation Mapping in the Himalayas of Uttarakhand and Himachal Pradesh states using remote sensing and GIS techniques. National Remote Sensing Agency, Department of Space, Hyderabad.

Onagh M, Kumra V K and Rai P K 2012 Landslide susceptibility mapping in a part of Uttarkashi district (India) by multiple linear regression method; *Int. J. Geol., Earth and Environ. Sci.* **2(2)** 102–120.

Ozdemir A and Altural T 2013 A comparative study of frequency ratio, weights of evidence and logistic regression methods for landslide susceptibility mapping: Sultan Mountains, SW Turkey; *J. Asian Earth Sci.* **64** 180–197.

Petley D 2012 Global patterns of loss of life from landslides; *Geology* **40(10)** 927–930.

Pradhan S P and Siddique T 2020 Stability assessment of landslide-prone road cut rock slopes in Himalayan terrain: A finite element method based approach; *J. Rock Mech. Geotech. Eng.* **12(1)** 59–73.

Ram P, Gupta V, Devi M and Vishwakarma N 2020 Landslide susceptibility mapping using bivariate statistical method for the hilly township of Mussoorie and its surrounding areas, Uttarakhand Himalaya; *J. Earth Syst. Sci.* **129(1)** 1–18.

Ram P and Gupta V 2021 Landslide hazard, vulnerability and risk assessment (HVRA), Mussoorie township, Lesser Himalaya, India; *Environ. Develop. Sustain.,* https://doi.org/10.1007/s10668-021-01449-2.

Sarkar S, Roy A K and Martha T R 2013 Landslide susceptibility assessment using information value method in parts of the Darjeeling Himalayas; *J. Geol. Soc. India* **82(4)** 351–362.

Sati S P, Naithani A and Rawat G S 1998 Landslides in the Garhwal Lesser Himalaya, UP, India; *Environmentalist* **18(3)** 149–155.

Sevgen E, Kocaman S, Nefeslioglu H A and Gokceoglu C 2019 A novel performance assessment approach using photogrammetric techniques for landslide susceptibility mapping with logistic regression, ANN and random forest; *Sensors* **19(18)** 3940.

Shano L, Raghuvanshi T K and Meten M 2020 Landslide susceptibility evaluation and hazard zonation techniques – a review; *Geoenviron. Disasters* **7** 1–19.

Sharma S and Mahajan A K 2019 A comparative assessment of information value, frequency ratio and analytical hierarchy process models for landslide susceptibility mapping of a Himalayan watershed, India; *Bull. Eng. Geol. Environ.* **78(4)** 2431–2448.

Solanki A, Gupta V, Bhakuni S S, Ram P and Joshi M 2019 Geological and geotechnical characterisation of the Khotila landslide in the Dharchula region, NE Kumaun Himalaya; *J. Earth Syst. Sci.* **128(4)** 1–14.

Tandon R S, Gupta V and Venkateshwarlu B 2021 Geological, geotechnical, and GPR investigations along the Mansa Devi hill-bypass (MDHB) Road, Uttarakhand, India; *Landslides* **18** 849–863, https://doi.org/10.1007/s10346-020-01546-9.

Thakur V C 1992 Geology of western Himalaya; *Phys. Chem. Earth* **19** 1–355.

van Westen C J, Castellanos E and Kuriakose S L 2008 Spatial data for landslide susceptibility, hazard, and vulnerability assessment: An overview; *Eng. Geol.* **102(3–4)** 112–131.

Yin K L and Yan T Z 1988 Statistical prediction models for instability of metamorphosed rocks; In: *Int. Symp. on Landslides* **5** 1269–1272.

Yu C and Chen J 2020 Landslide susceptibility mapping using the slope unit for southeastern Helong City, Jilin Province, China: A comparison of ANN and SVM; *Symmetry* **12(6)** 1047.